Civil Engineering Infrastructures Journal 2022, 55(2): 293-307
DOI: 10.22059/CEIJ.2022.324782.1758

RESEARCH PAPER

On Compressive Stress-Strain Behavior of Standard Half-Scale Concrete Masonry Prisms

Kahrizi, E.[1], **Aghayari, R.**[2*], **Bahrami, M.**[3] **and Toopchi-Nezhad, H.**[2]

[1] M.Sc., Department of Civil Engineering, Razi University, Kermanshah, Iran.
[2] Associate Professor, Department of Civil Engineering, Razi University, Kermanshah, Iran.
[3] Ph.D. Candidate, Department of Civil Engineering, Razi University, Kermanshah, Iran.

Received: 30 May 2021; Revised: 29 Sep. 2021; Accepted: 11 Oct. 2021

ABSTRACT: Masonry buildings are the most utilized structural system worldwide due to the ease of construction and cost-effectiveness. The effective design of masonry structures has been always an important research subject. Experimental studies are the main component of such research studies. The budget and equipment limitations may challenge the laboratory testing of full-scale masonry specimens and test structures. As such, the use of model-scale specimens may be found as a promising alternative to study the response behavior of this type of structure. In this paper, the stress-strain behavior of half-scale concrete masonry units and prisms (hollow and fully grouted) under compressive loads is evaluated and compared with their full-scale counterparts. The half-scale specimens are standard in that the principles of similitude law have been followed precisely in their aggregate grading, mix-design, physical dimensions, and loading. The stress-strain diagram and failure modes of the half-scale are similar to those of the full-scale. The ratio of half-scale to the full-scale compressive strength of the hollow and grouted masonry prisms on average was found to be 1.07, and 1.08, respectively. The experimentally-evaluated response of the standard half-scale specimens that fully satisfy the requirements of similitude law may be extended with good accuracy to the full-scale masonry.

Keywords: Compression Test, Concrete Masonry, Prism Testing, Small-Scale Modeling.

1. Introduction

Masonry structures comprise a large portion of building inventory worldwide. Masonry buildings incorporate load-bearing walls that perform a variety of other functions in addition to supporting the loads. The load-bearing walls in a masonry building subdivide spaces, provide thermal and acoustic insulation, and provide fire and weather protection. These functions in a framed building have to be accounted for separately (Rai, 2002). Other advantages such as the possibility of using local labor and materials, ease of construction, longevity, being architecturally pleasant, and cost-effectiveness have made this type of structure a suitable choice for many

* Corresponding author E-mail: reza_agh@razi.ac.ir

projects.

Masonry buildings may be constructed with stones, bricks, and concrete blocks. Stones have been frequently employed in the construction of historic buildings. Many old buildings were built with unreinforced brick- or block-masonry. Being unreinforced, the masonry assemblages in such buildings are very susceptible to brittle failure during seismic events.

The engineering design of masonry buildings dates back to the 1950s, where, intensive theoretical and experimental research studies were conducted on various aspects of masonry subassemblies (Rai, 2002). The contemporary masonry structures incorporate steel reinforcement to improve the flexural and shear behavior of the walls under earthquake loads. The design is conducted based on the factors affecting the strength, stability, and hysteretic load-displacement performance of masonry structures. Current masonry code provisions may be divided into two broad categories, namely, empirical design methods, and strength design methods (ACI 530, 2013; CSA Standard A165, 2002; Eurocode 6-1996-1-1, 1996-3, 2006).

The empirical design includes a set of construction criteria that is applied to the buildings of specific constraints. For instance, to achieve an intermediate level of ductility in the unreinforced masonry buildings, the load-bearing masonry walls may be confined with a set of horizontal and vertical reinforced-concrete tie-elements based on empirical guidelines (Standard No. 2800, 2013). The tie-elements which are mainly constructed at the intersection of perpendicular walls and the roof levels, also improve the monolithic performance of the whole building. The design of this structural system is empirical with no engineering calculations to evaluate the demand and capacity of the walls. As such, the mechanical properties of the masonry units and mortar are not directly taken into account during the design process and detailing of the structure. The number of above-ground stories in this system is limited to two stories only (Standard No. 2800, 2013). The tied-masonry buildings performed satisfactorily in the past moderate earthquakes of Iran (Eshghi et al., 2009).

The strength design methods in modern design codes such as ACI 530, CSA A371, and Eurocode 6 are based on the ultimate- or limit-state-design methodologies. The design steps include the loading of structure, structural analysis, and design. The analysis is carried on the structural model of the building which can be created in many commercial software packages. The analysis outputs represent the demands on different structural elements of the masonry building. The load-capacity of the walls including, axial, in-plane and out-of-plane flexural, and shear strength values are determined based on the code-specified expressions, and the nominal mechanical properties of masonry units and prisms. The design objective is to match the capacities with the demands.

As with the other structural systems, the design code regulations for masonry buildings are being developed continuously. This is evidenced by the changes taking place in the masonry codes internationally (Rai, 2002). A significant number of studies on the compressive behavior of hollow, partially-grouted, and fully-grouted concrete masonry assemblages can be found in the literature. These studies investigated the influence of different parameters including block compressive strength, type of mortar and grout, the number of vertical and horizontal mortar joints within the specimen, mix design, and water to cement ratio on the compressive strength and failure modes of full-scale masonry assemblages (Zahra et al., 2021; Hassanli et al., 2015; Mohammad et al., 2010; Andria, 2017; Huang et al., 2017; Oliveira et al., 2014; Gustavo 2019).

Experimental studies are a major prerequisite to code developments. However, the cost of testing on full-scale masonry specimens and systems is prohibitive (Hamid et al., 1985). Working on model-scale specimens and structures is a rational way of cutting the costs of experimental studies. Hamid et al. (1985) studied the effects of mortar and grout strength, height-to-thickness ratio, number of courses, and bond type on the ¼ scale prism compressive strength. According to the authors, excellent correlations were obtained for the mode of failure and moduli of elasticity of ¼ scale and full-scale prisms. Another study on the ¼ scale concrete masonry prisms showed the relatively higher compressive strength of the full-scale prisms (Camacho et al., 2000). Long et al. (2005) studied the compressive strength and diagonal tension of ½ scale masonry prisms. They concluded that the half-scale masonry could be deemed as a good model of full-scale masonry, particularly for grouted specimens. Another study on ½ scale masonry prisms showed a comparable modulus of elasticity and strain at peak strength to their full-scale counterparts, and some discrepancies in the compressive strength and post-peak behavior (AbdelRahman et al., 2020). Sathiparan et al. (2016) studied the effects of scale on the mechanical properties of concrete blocks and prisms and concluded that while the compressive strength of masonry did not significantly influence by the scale, all of the other tested properties, including water absorption rate, porosity, shear strength, and flexural bond strength significantly influenced by the scale.

Given the disparate results found in the literature on the effects of the scale of the behavior of concrete masonry, this field deserves further investigation. The main objective of this study is to construct standard ½ scale concrete masonry prisms to be the most representative of their full-scale counterparts under compressive loads. This is however conditional on following the principles of true similitude law in the construction of the model-scale masonry units and specimens. The similitude law that is employed in this study is known as the “practical true model” (Harris et al., 1999). This is an appropriate modeling technique that is used to study the elastic and inelastic behavior and failure modes of masonry structures to static loads under the assumption that there are no significant time-dependent effects that influence the structural behavior. In this similitude model, the material properties are the same in both model and the prototype (i.e., the full-scale model) structure. For complete similarity of the structural behavior, a dimensional analysis will give the scale factors shown in Table 1. The length scale factor, S_l, in a half-scale model is $\frac{1}{2}$. If it is assumed that the stresses caused by the self-weight of the structure are not significant, as is the case for most masonry buildings, the scale factors cited in Table 1 are adequate for modeling masonry structures (Harris et al., 1999).

Table 1. Scale factors in the practical true model (Harris et al., 1999)

Quantity	Dimension	Scale factor
Linear dimension	L	S_l
Area	L^2	S_l^2
Concentrated load	F	S_l^2
Pressure	FL^{-2}	1
Displacements	L	S_l
Stress	FL^{-2}	1
Strain	1	1
Specific weight	FL^{-3}	$1/S_l$

In this study, the principles of similitude law have been followed precisely in the grading of aggregate, mix-design, physical dimensions of the blocks, and loading of the half-scale masonry blocks and prisms and their corresponding full-scale counterparts.

2. Experimental Program

The main purpose of this research is to investigate the relationship between mechanical properties, and the load-deformation behavior of half-scale and full-scale masonry prisms; material and laboratory conditions in both scales are identical and made under ASTM standards.

Therefore, in the first step, the physical and mechanical properties of half-scale and full-scale masonry blocks were evaluated and compared. In the second phase of the study, the hollow and grouted masonry prisms were constructed in half-scale and full-scale, and then their mechanical properties, as well as their stress-strain diagrams, were evaluated and compared.

2.1. Test Specimens

2.1.1. Dimensions of Concrete Blocks

Figure 1 shows the typical hollow concrete blocks fabricated for this study. As seen, the masonry blocks are Full-Scale (FS) and Half-Scale (HS) splitter units with the physical dimensions outlined in Table 2. The physical dimensions including the thicknesses of face-sell and web of the FS-units satisfy the minimum requirements prescribed by the ASTM C90.

As seen in Table 2, the HS-blocks represent a true half-scale replica of their full-scale counterparts.

2.2. Mix Design for Full-Scale Concrete Blocks

Proportioning the mix components for a Concrete Masonry Unit (CMU) is an important step in producing high-quality units. A well-proportioned mix will result in improved mechanical properties (such as compressive strength, weight, and absorption rate of the masonry unit). As a preliminary step, a well-graded aggregate must be selected for the concrete mix. In this study, the aggregates of the concrete mix were graded based on ASTM C136M, guidelines using sieve analysis. Figure 2 shows the distribution of particles in the granular material (i.e., results of the sieve analysis). The upper and lower bounds prescribed by the ASTM C136 are also shown in the figure.

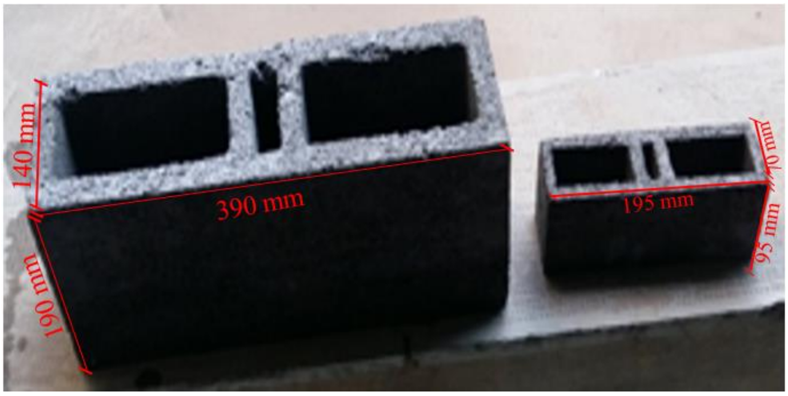

Fig. 1. Typical concrete masonry unit (full-scale and half-scale)

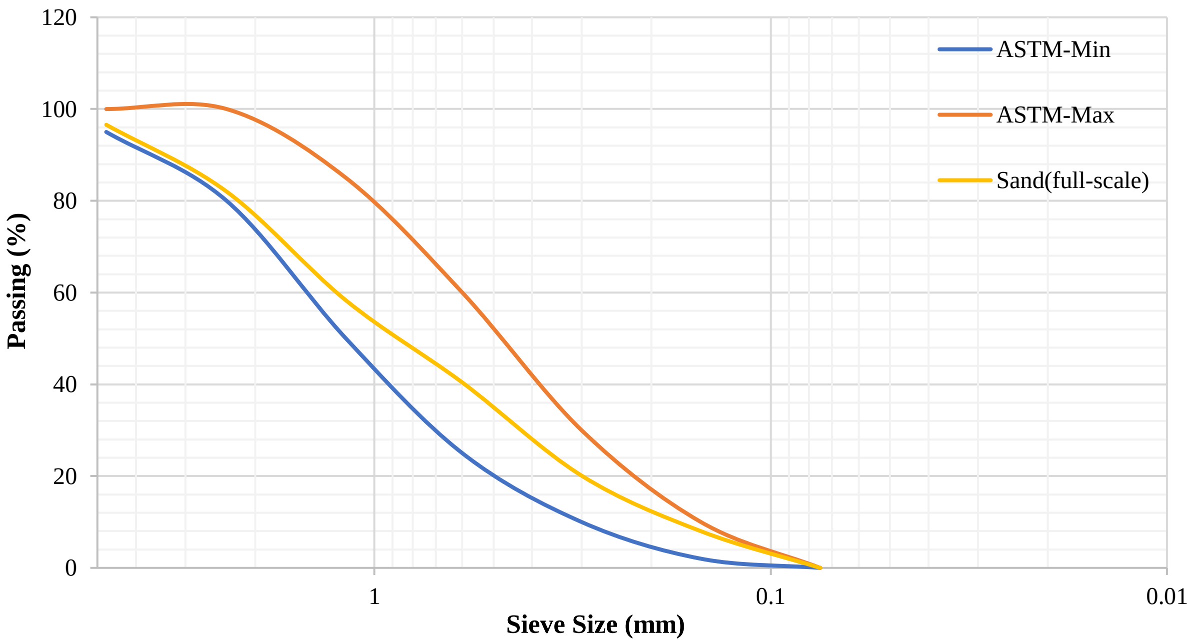

Fig. 2. Grading of aggregates for the full-scale blocks

Table 2. Physical dimensions of concrete masonry units

Scale	Length (mm)	Heigth (mm)	Width (mm)	Face shell thickness (mm)	Web thickness (mm)	Solid (%)
Half	195	95	70	14	11	53.48%
Full	390	190	140	28	22	53.48%

The concrete mix of the masonry units contains both fine-grained and coarse-grained materials (25% gravel and 75% sand). The gravel material of the concrete mix passed Sieve #3/8 and remained on Sieve #4 as prescribed by the ASTM C136. In additional Cement is one of the most extensively used construction material for buildings and infrastructures in Iran (Hosseinijou et al., 2021), in concrete mix of blocks were used cement type II.

The fineness modulus (FM) method is one of the most commonly used techniques to design the concrete mix for masonry units (Jablonsky, 1996). To obtain an optimal-mix design, the concrete blocks of different water, cement, and aggregate weight ratios were fabricated and tested for compressive strength. The compressive strength is determined by dividing the ultimate compressive force by the net area of the concrete block. The net area is calculated by dividing the net volume of the masonry unit by its total height. The net volume is evaluated based on the procedure outlined in the ASTM C140-13. To eliminate any inconsistency in the test results, the top and bottom surfaces of the masonry blocks were capped with a thin layer of high-strength gypsum with an approximately 2 to 3 mm thickness.

A total of eight different mix designs were investigated in this study (see Table 3). According to the ASTM C90, the lower admissible grade for the structural concrete blocks is 13.1 MPa. Accordingly, the mix designs 5 to 8 that comply with this requirement may be deemed acceptable (see Table 3). Given the larger strength of the mix-design 7, it was selected for the fabrication of the concrete blocks of this study.

According to the numbers in the last column of Table 3, Mix design 7 is acceptable and optimal.

2.3. Mix Design for Half-Scale Concrete Blocks

The Half-Scale (HS) blocks are designed and fabricated based on a true replica model in which the material properties of the model remain the same as those of the full-scale model. However, the physical dimensions of the model scale block, as well as its granular aggregates, are scaled by a factor of ½.

To achieve a well-graded half-scale aggregate consistent with the full-scale granular materials, the sieve size of the upper and lower bounds of the ASTM C136 shown in Figure 2 were multiplied by the scale factor of ½.

Thus, the maximum size of the half-scale aggregates was selected to be 2.38 mm that was half of the maximum size of 4.75 mm in the full-scale aggregates. Figure 3 shows the distribution of particles in the granular material (results of sieve analysis) and the upper and lower bounds prescribed by ASTM C136 that were multiplied by the scale factor of ½.

Table 3. Mix design of the concrete blocks

Mix designs	The weight ratio of cement to aggregate	The weight ratio of water to the mixture of cement and aggregate	Water to cement ratio	Average compressive strength of 3 block at 28 says (MPa)
1	1:9	7.5%	0.75	9.4
2	1:8	7%	0.63	9.5
3	1:7	7%	0.56	12.3
4	1:6	7.5%	0.54	10.36
5	1:6	7%	0.49	13.3
6	1:5	8.3%	0.5	17.2
7	1:5	8.1%	0.49	18.1
8	1:4	8.8%	0.44	14.1

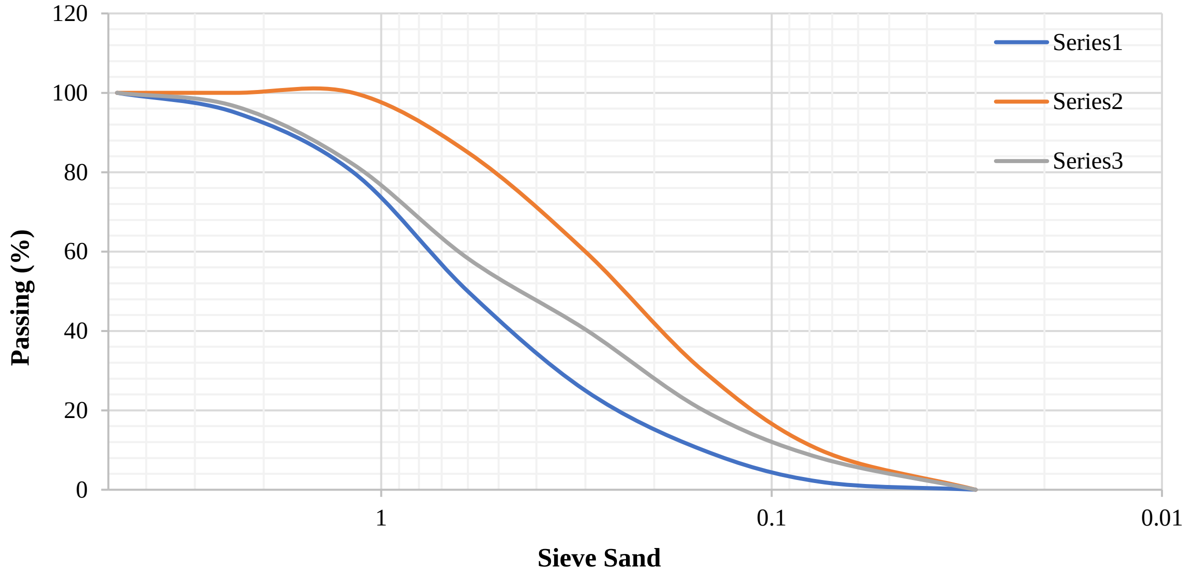

Fig. 3. Grading of aggregates for the half-scale blocks

The half-scale aggregates were employed in a mix-design consistent with the mix-design 7 given in Table 3. Three HS-blocks were fabricated and tested in conformance with ASTM C90. The average compressive strength of the said HS-blocks was measured to be 17.9 MPa which was in excellent agreement with the compressive strength of 18.1 MPa obtained for the FS-blocks.

3. Material Properties of the Concrete Blocks

The density, water absorption, and linear shrinkage are the critical material properties that are used, in addition to the compressive strength, to classify the concrete masonry units. Table 4 includes the average values of the said material properties for the full-scale and half-scale concrete blocks. The concrete block density is evaluated based on ASTM C90. The masonry blocks are classified as heavy-, normal-, and light-weight depending on the density of the concrete material. Given the average density evaluated for the masonry blocks of this study, both the FS- and HS-concrete blocks may be classified as normal-weight. The level of water absorption of concrete is evaluated experimentally in conformance with ASTM C140. As seen in Table 4, the absorption values evaluated for the FS- and HS-blocks satisfied the maximum permissible value outlined by the relevant ASTM standard. The linear shrinkage of the concrete material was evaluated with the aid of ASTM C426.

The mechanical properties of the concrete blocks were determined according to ASTM C90 guidelines. Using Archimedes' law, the volume of the full-scale and half-scale blocks was evaluated to be 0.005538 and 0.000692 m^3, respectively. As such, the effective cross-sectional area of the full-scale and half-scale blocks (determined by dividing the volume by the total height of the block) was evaluated to be 29147.4 and 7284 mm^2, respectively. The ratio of the half-scale to full-scale cross-section areas read 0.25, which is consistent with the square of the scale factor, i.e., $(½)^2 = 0.25$.

The last column of the table shows the ratio of half-scale to full-scale of the mechanical properties evaluated for the masonry blocks of this study. As seen, an excellent correlation exists between the two. The largest difference is related to the absorption of the blocks. The level of absorption is proportional to the perimeter surface of the block. The perimeter surfaces of the full-scale and half-scale blocks were measured to be 411920 and 102980 mm^2, respectively. The ratio of half-scale to full-scale perimeter two areas is 0.25.

Table 4. Material properties of concrete masonry units (full-scale and half-scale)

Property	Half-scale (Average)	Full-scale (Average)	ASTM-req	(Half-scale/ Full-scale)
Density (kg/m^3)	2020.23	2133.38	Normal weight[1]	0.95
Absorption (kg/m^3)	143.86	168.8	208 kg/m^3	0.85
Compressive strength (MPa)	17.47	17.6	≥ 13.1	1.01
Linear shrinkage	0.19%	0.18%	≤ 0.065% [4]	1.05

1: According to ASTM C90, as the density of half-scale and full-scale blocks was greater than 2000 kg/m^3, both blocks were classified as normal weight blocks.
2: ASTM C140, the Maximum Absorption averaged three normal weight blocks is 208 kg/m^3
3: ASTM C90, Minimum compressive strength averaged three normal weight blocks is 13.1 MPa
4: ASTM C90 limits its potential drying shrinkage to 0.065%.

4. Mortar and Grout

4.1. Full-Scale Masonry

The sand grading for the preparation of mortar (type S) and grout is based on the ASTM C144 and ASTM C404 requirements, respectively. Figure 4 shows the results of sand grading, as well as the permissible bound recommended by the ASTM standard. As seen, overall, the sand grading satisfies the standard requirements.

According to the ASTM C270 the relative volume of cement, crushed lime, and sand in S mortar are recommended to be 1.5, 0.5, and 4.5, respectively. Besides, the compressive strength of standard samples of 100 × 100 × 100 mm is 12.4 MPa. Table 5 includes the strength values obtained for six mortar specimens. The average strength value is approximately 24 MPa.

Grout for use in concrete masonry construction should comply with ASTM C476. According to this standard relative volume of cement and sand is recommended to be 1 and 3, respectively. Also, the minimum grout compressive strength is 13.79 MPa. The average strength value obtained for six grout specimens is approximately 22.68 MPa.

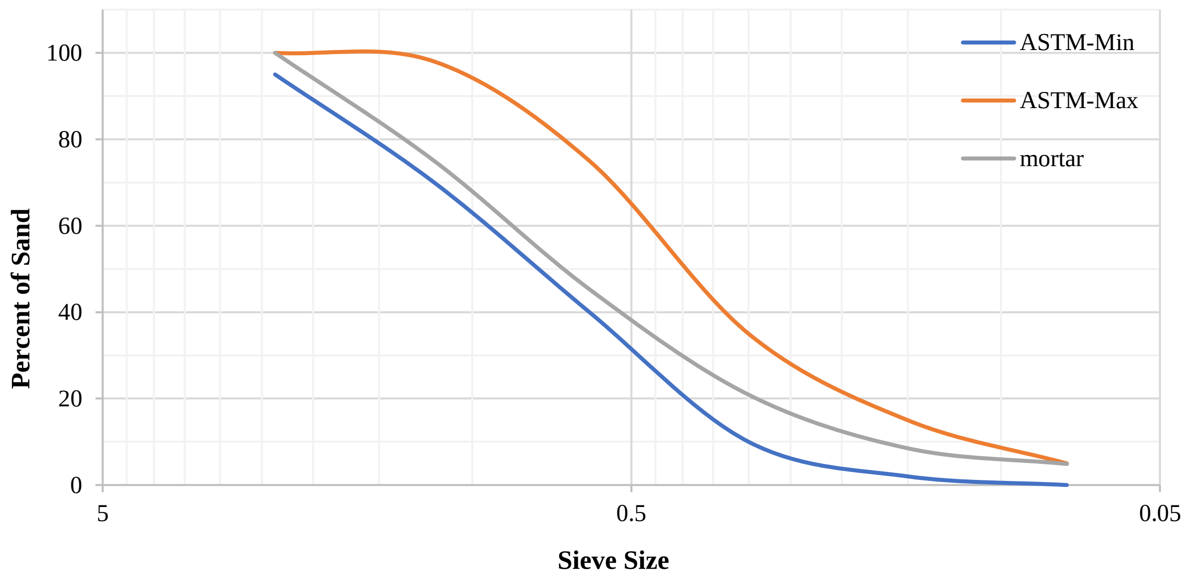

Fig. 4. Sand-grading for the (full-scale) mortar/grout

Table 5. Compressive strength of full-scale mortar specimens

Sample	1	2	3	4	5	6
Compressive strength (MPa)	24.06	27.04	25.43	22.87	21.59	23.45
Ave. strength (MPa)			24.07			

4.2. Half-Scale Masonry

In the construction of the half-scale units, both the physical geometry of the concrete block and the maximum size of its coarse aggregate were multiplied by a scale factor of ½. Consistently, in the mortar mix of the half-scale units, the maximum size of the coarse aggregate must be divided by a factor of 2. For the full-scale units, the sand material passing Sieve #8 was employed in the mortar mix design in conformance with the ASTM Standard. Therefore, to construct a consistent mortar mix for the half-scale units, the sand material passing Sieve #16 was utilized. Table 6 includes the compressive strength values obtained for the half-scale mortar cube specimens tested in conformance with ASTM C270. As with the full-scale specimens, the cubic half-scale mortar specimens were cured in a water pool for 28 days.

The average compressive strength of the full-scale and half-scale mortar specimens of this study were evaluated to be 24.1 MPa and 23.3 MPa, respectively. As such, the ratio of half-scale to the full-scale compressive strength of the mortar specimens was evaluated to be 0.97. The proximity of this ratio to the unity verifies the excellent consistency between the half-scale and full-scale mortar specimens.

As with mortar, half-scale grout specimens, the maximum size of the coarse aggregate and dimensions of samples must be divided by a factor of $^1/_2$, the cubic half-scale grout specimens were cured in a water pool for 28 days.

The average compressive strength of the full-scale and half-scale grout specimens was evaluated to be 22.68 MPa and 22.45 MPa, respectively. As such, the ratio of half-scale to the full-scale compressive strength of the grout specimens was evaluated to be 0.99.

5. Masonry Prisms

One of the main objectives of this research is to compare the compressive stress-strain properties of half-scale and full-scale concrete masonry prisms. As such, a set of hollow and fully grouted masonry prisms were constructed in full- and half-scale arrangements. The compressive strength of the prisms was evaluated experimentally according to the CSA A165. According to this standard, the prism specimens comprise four courses of concrete blocks, three rows of mortar bed joints, and two mortar head joints as seen in Figure 5. Results of such specimens are more representative of a real concrete masonry wall as they include the influence of both the mortar bed joints and head joints in the compressive behavior of the masonry assemblage. The width of mortar joints in the full-scale and half-scale masonry prisms was 10 mm and 5 mm, respectively. To eliminate any inconsistency in the test results as a result of stress concentrations, the top and bottom surfaces of the masonry prisms were capped with a thin layer of 2 to 3 mm thickness of high-strength gypsum (see Figure 5). All of the prisms were tested after 28-days.

5.1. Test Setup

Figure 6 shows an overview of the test setup. As seen in this figure the masonry prism is placed between the rigid upper and lower platens of the test machine**.**

The compressive load is measured via a load cell secured between the upper platen and the hydraulic ram. The test is performed in a displacement control manner. The outputs of a linear potentiometer that provided the feedback signals to manage the motions of the ram, was utilized as the vertical deformations of the masonry prism.

5.2. Test Results

In this study 20 masonry prisms in two groups were tested. Each group contains 5 grouted and 5 ungrouted masonry prisms. The ultimate compressive load, P, and ultimate strength, f'_m of the prisms of this study are summarized in Table 7. The ultimate strength of masonry prisms was calculated by dividing the ultimate load by the effective cross-section of the prisms.

Table 6. Compressive strength of full-scale mortar specimens

Sample	1	2	3	4	5	6
Compressive strength (MPa)	24.06	27.04	25.43	22.87	21.59	23.45
Ave. strength (MPa)	24.07					

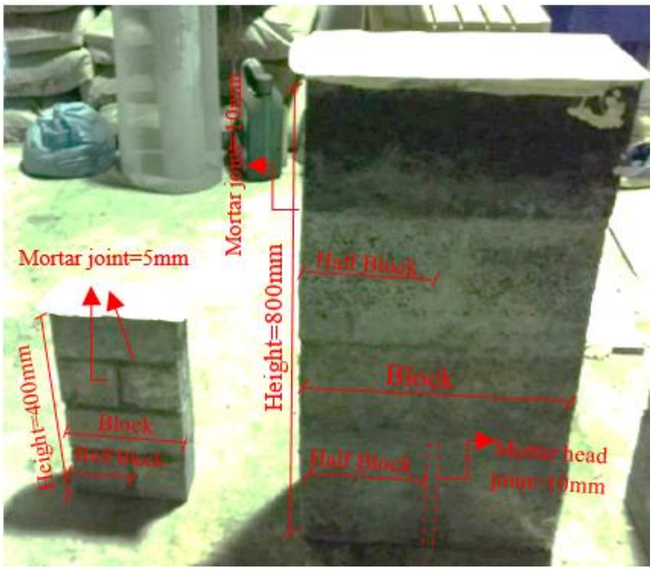

Fig. 5. Typical half-scale and full-scale masonry prisms


Fig. 6. An overview of the compression test setup for the masonry prisms

According to ASTM C1314, the ultimate strength of the masonry prism must be modified to include its slenderness ratio. The correction factor is determined based on the ratio of height, h_p, to thickness (the smallest dimension of the masonry prism), t_p, according to the following table (ASTM C140).

The correction factors shown in Table 7 may be linearly interpolated for the h_p/t_p values are not given directly in the table. However, the correction factors may not be extrapolated for the aspect ratios 1.3 and 5.0. Given the height to thickness ratio of the masonry prisms, 5.6, the correction factor from Table 7 is evaluated to be 1.22. This correction factor was applied to the ultimate compressive strength values given in Table 8. Table 8 also includes the average and standard deviation of the results. The ratio of the standard deviation to the mean (average) of the strength values, f'_m, ranges from 6.8% to 8.4% in different prisms. The relatively low standard deviation values indicate that the results are not widely dispersed about the average values.

Table 7. Height to thickness correction factors for masonry prism compressive strength (ASTM C140)

h_p/t_p	1.3	1.5	2	2.5	3	4	5
Correction factor	0.75	0.86	1	1.04	1.07	1.15	1.22

Table 8. Results of axial compression tests for the full-scale and half-scale prisms

prism	Hollow					Grouted				
	Half-Scale (HS)		Full-Scale (FS)		$\frac{f'_{m,HS}}{f'_{m,FS}}$	Half-Scale (HG)		Full-Scale (FG)		$\frac{f'_{m,HS}}{f'_{m,FS}}$
	P (kN)	$^*f'_m$ (MPa)	P (kN)	f'_m (MPa)		P (kN)	f'_m (MPa)	P (kN)	$^*f'_m$ (MPa)	
1	81.90	17.08	286.45	14.93	1.14	170.17	15.2	528.89	11.81	1.28
2	90.45	18.86	345.90	18.03	1.05	154.25	13.78	647.82	14.48	0.95
3	75.10	15.66	331.45	17.27	0.90	145.01	12.97	588.59	13.15	0.99
4	87.08	18.16	293.70	15.30	1.18	185.97	16.61	592.75	13.24	1.25
5	96.72	20.17	361.19	18.82	1.07	142.88	12.77	586.7	13.11	0.97
Ave.	**84.33**	**18.06**	**326.89**	**16.87**	**1.07**	**159.66**	**14.26**	**588.95**	**13.16**	**1.08**
St. Dev.	**2.76**	**1.23**	**5.41**	**1.23**	**0.30**	**1.27**	**1.20**	**6.08**	**0.92**	**0.37**

$*f'_m = \frac{(\text{Correction Factor}(Table 6) \times P)}{A_e}$

In the construction of the masonry prisms of this study, the S-mortar was only applied to the webs (side walls) of the concrete blocks. Therefore, the effective cross-section in the hollow prisms of this study is equivalent to the cross-section of the block webs. The effective cross-section area for the full-scale and half-scale hollow prisms are 2 × 390 × 30 = 23400 mm^2, and 2 × 195 × 15 = 5850 mm^2, respectively. The effective cross-section area in the grouted specimens is calculated to be 390 × 140 = 54600 mm^2, and 195 × 70 = 13650 mm^2, for the full-scale and half-scale prisms, respectively.

The ultimate strength of a masonry assemblage is affected by the compressive strength of its masonry units and the type of mortar used in its construction. Given the compressive strength of the concrete blocks of this study, the minimum ultimate compressive strength of a concrete masonry prism constructed with Type S mortar is expected to be 11.5 and 8.8 for hollow and grouted prisms, respectively, based on CSA A165. According to Table 8, the minimum compressive strength of the full-scale for hollow and grouted prisms are 14.93 and 11.81 MPa, respectively. These values are comparable with the strength values prescribed by the CSA A165 standard. The lower compressive strength of the grouted prisms as compared to the hollow prisms is related to the effects of several factors including the water absorption of the concrete masonry units and the grout shrinkage (Drysdale et al., 1994). Although grouting results in reduced compressive strength, the larger effective cross-section area of the grouted masonry prism results in an increased compressive load-bearing capacity as compared to its hollow prism counterpart.

For the hollow and grouted masonry prisms, the ratio of half-scale to full-scale compressive strength values was evaluated to be 1.07, and 1.08, respectively. These indicate the excellent consistency that exists between the half-scale and full-scale prisms of this study. The average stress-strain curves obtained for the hollow and grouted prisms are shown in Figures 7a and 7b, respectively. The following procedure used to obtain the average stress-strain curves shown in Figure 7. First the experimental stress-strain curve of the individual specimens of each group of prisms were evaluated. Next, a polynomial of order 6 was fitted to each curve, and its coefficients were evaluated with a double precision accuracy (This was performed in excel). For each specimen the magnitude of the corresponding stress at any desired strain level could be calculated using the polynomial function evaluated specifically for that specimen in the previous step. The average stress-strain curve was constructed by calculating the average stress values of specimens at various discrete strain levels.

Figure 7 contains the stress-strain curves of the full-scale and half-scale specimens. Overall, a reasonable correlation exists between the stress-strain relationships of the full-scale and half-scale prisms. The average ultimate strength of the half-scale hollow and grouted prisms to their full-scale counterparts was found to be 107% and 108%, respectively.

Given the nonlinear stress-strain behavior of masonry prisms, the secant modulus of elasticity varies with the magnitude of stress (or strain) values experienced by the material. In this study, the chord modulus of elasticity as a material property of the prisms was evaluated and compared. The chord modulus of elasticity represents the slope of a line fitted to the stress-strain curve between the stress values ranging from 5% to 33% of the compressive strength of prisms (Drysdale et al., 1994). Table 9 includes the average chord modulus of elasticity of the prisms. The last column of the table indicates the ratio of half-scale to full-scale moduli. As seen an acceptable correlation exists between the model and prototype masonry prism. The fully grouted prisms show better consistency.

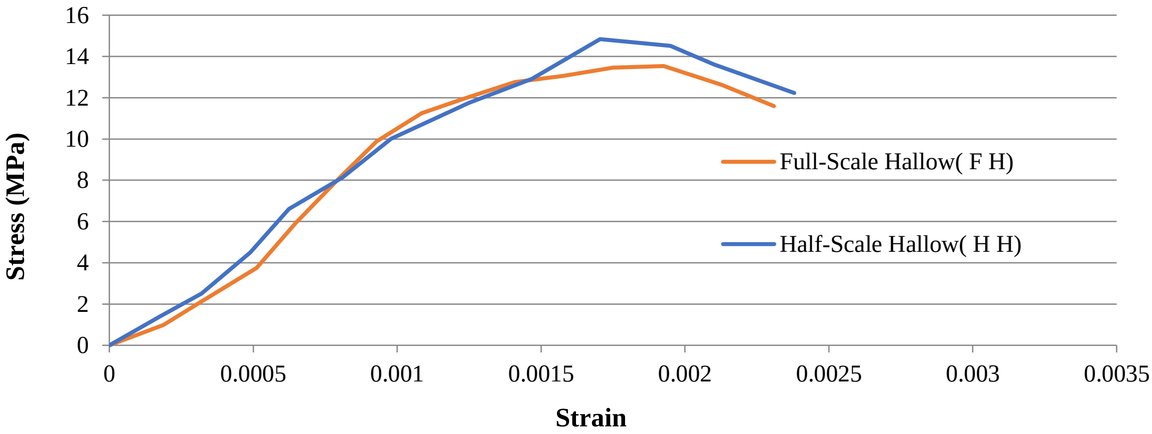

(a) Hollow Prisms

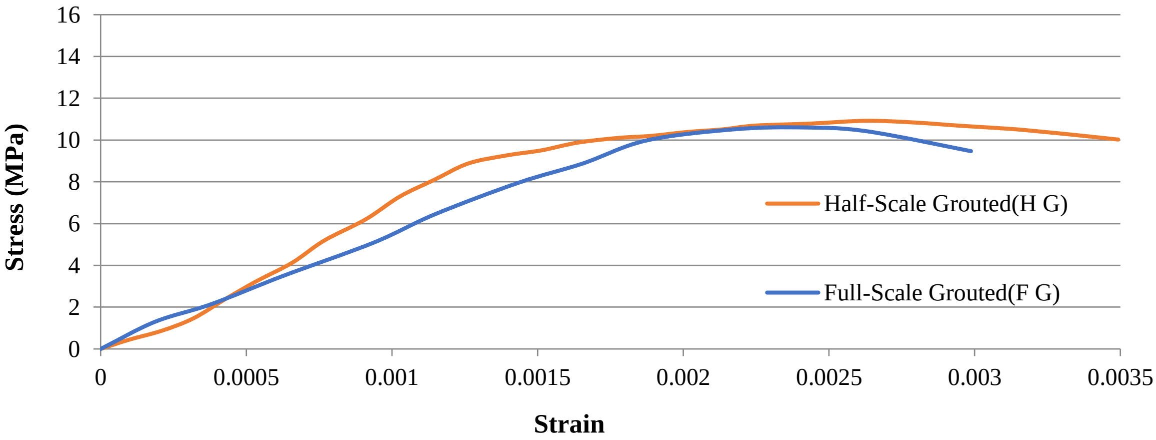

(b) Grouted Prisms

Fig. 7. Stress-strain curves of full-scale and half-scale masonry prisms

Table 9. The chord modulus of elasticity of the masonry prisms

Prism		σ_{Max}	$0.33\sigma_{Max}$	$\varepsilon_{0.33\sigma Max}$	E (MPa)	$\frac{E_{Half-Scale}}{E_{Full-Scale}}$
Hollow prism	HH	14.8	4.88	0.00055	8872	1.17
	FH	13.8	4.55	0.0006	7590	
Grouted prism	HG	11.7	3.86	0.0006	6433	1.12
	FG	10.8	3.56	0.00062	5748	

Figure 8a shows the typical failure modes observed in the full-scale hollow prisms (FH) after the completion of testing. The failure pattern includes the formation of significant vertical cracks, (along the axis of compression loading) in the webs of the concrete blocks, as well as in the mortar head joints of the prism. The face shells of the concrete blocks would also experience significant cracks and failure. According to Figure 8b, a relatively similar pattern of failure was observed in the hollow half-scale (HH) prisms.

Figure 9a shows the pattern of failure in the full-scale grouted (FG) prisms. Unlike the hollow prisms, no visible distress was observed in the specimen before the axial load reached its maximum value. When the axial load converged to its ultimate value, the vertical cracks initiated at the sides of the prism. The cracks were expanded and enlarged by increasing axial load. Eventually, the horizontal cracks that led to the splitting of the masonry assemblage were created. The failure pattern of the half-scale grouted (HG) prisms was found to be similar to that of the full-scale specimens (see Figure 9b).

(a) Typical failure modes in the FH

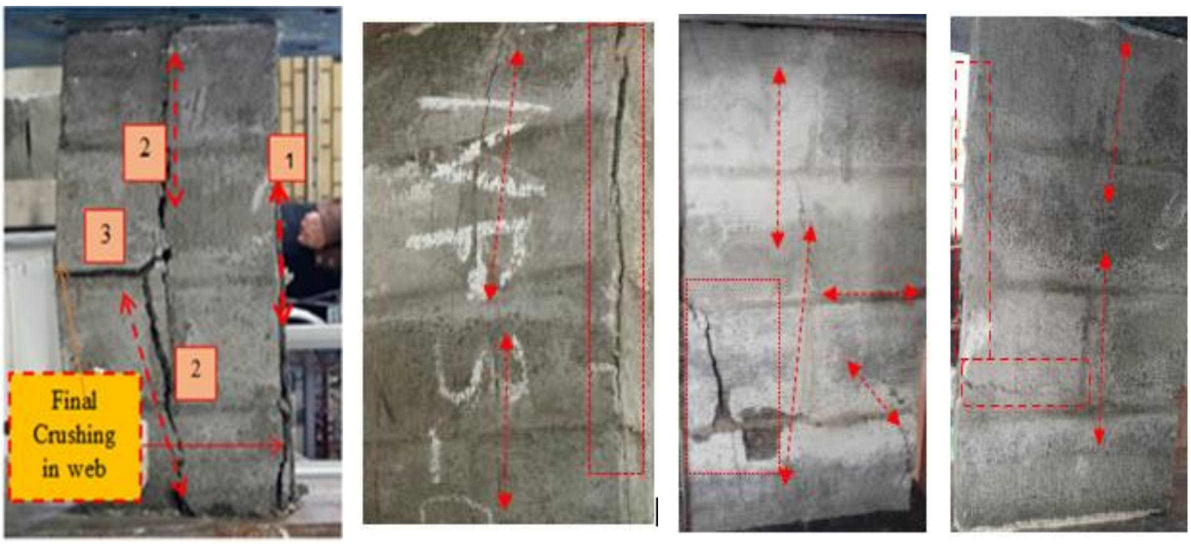

(b) Typical failure modes in the HH

Fig. 8. Typical failure modes in the FH and HH prisms

(a) Typical failure modes in the FG

(b) Typical failure modes in the HG

Fig. 9. Typical failure modes in the FG and HG prisms

6. Conclusions

In this research, the stress-strain behavior of the full-scale and half-scale concrete masonry blocks and prisms were investigated experimentally. The objective was to construct half-scale masonry units and prisms to be a true replica of the conventional full-scale counterparts. To achieve the research objectives, the size of aggregates in the concrete, mortar, and grout mixes, and the physical dimensions of the half-scale masonry assemblages complied with the scale-factor of ½ according to the similitude law. The ultimate strength of the half-scale specimens was evaluated and compared with those of the full-scale configuration. The main outcomes of this study are as follows:

Masonry units: The ratio of half-scale to full-scale mass density, water absorption, and linear shrinkage were measured to be 0.95, 0.85, and 1.05, respectively. The compressive strength of the half-scale unit was found to be on average nearly 1% larger than the full-scale blocks.

Mortar and grout: The ratio of half-scale to the full-scale compressive strength of the grout and mortar specimens was evaluated to be 0.99 and 0.97, respectively.

Masonry prisms: The ultimate compressive strength of the half-scale hollow masonry prisms was found to be on average 7% larger than their full-scale counterparts. Similarly, the average ultimate strength of the half-scale fully-grouted prisms was +8% off as compared to their corresponding full-scale prisms. The chord modulus of elasticity of half-scale hollow and grouted specimens was found to be on average 17% and 12% larger than their corresponding full-scale specimens, respectively. As such, the half-scale prisms were found to be slightly stronger and stiffer than the full-scale ones under compressive loads due to the scale effects. The failure modes of the two systems were found to be similar.

The results of this study suggest that the standard half-scale units and assemblages that are constructed consistent with the principles of similitude law are to a large extent representative of the response behavior of the full-scale masonry units and assemblages. As such, the response behavior of the half-scale concrete masonry assemblages may be extended to the conventional full-scale masonry specimens. This conclusion is of interest as the application of standard half-scale masonry units in experimental research studies leads to significant ease of work and cost savings.

7. References

AbdelRahman, B. and Galal, K. (2020). "Influence of pre-wetting, non-shrink grout, and scaling on the compressive strength of grouted concrete masonry prisms", *Construction and Building Materials*, 241, 117985.

ACI 530. (2013). *Building code requirements and specification for masonry structures and companion commentaries*, American Concrete Institute.

Alvarenga, R.C.S.S., Nalon, G.H., Fioresi, L.A.F., Pinto, M.C., Pedroti, L.G. and Ribeiro, J.C.L. (2017) "Experimental evaluation of the influence of mortar's mechanical properties on the behavior of clay masonry", In *Characterization of Minerals, Metals, and Materials*, 2017, 671-679, Springer, Cham.

Andria, I., Samira, R., Mark, H., Pedram, K. and Nigel, SH. (2017). "Testing and finite element modeling of concrete block masonry in compression", *13th Canadian Masonry Symposium*, Halifax, Canada.

ASTM C90-16a. (2016). *Standard specification for loadbearing concrete masonry units*, American Society for Testing and Materials, West Conshohocken, Pa.

ASTM C136/C136M-19. (2019). *Standard test method for sieve analysis of fine and coarse aggregate*, American Society for Testing and Materials, West Conshohocken, Pa.

ASTM C140-13a. (2013a). *Standard test methods for sampling and testing concrete masonry units and related units*, American Society for Testing and Materials, West Conshohocken, Pa.

ASTM C144-04. (2018). *Standard specification for aggregate for masonry mortar*, American Society for Testing and Materials, West Conshohocken, Pa.

ASTM C270-19. (2019). *Standard specification for mortar for unit masonry*, American Society for Testing and Materials, West Conshohocken, Pa.

ASTM C426-16. (2016). *Standard test method for linear drying shrinkage of concrete masonry units*, American Society for Testing and Materials, West Conshohocken.

ASTM C404-18. (2018). *Standard specification for aggregates for masonry grout*, American Society for Testing and Materials, West Conshohocken, Pa.

ASTM C476-19. (2019). *Standard specification for grout for masonry*, American Society for Testing and Materials, West Conshohocken, Pa.

ASTM C1314-12. (2012). *Standard test method for compressive strength of masonry prisms*, American Society for Testing and Materials, West Conshohocken, Pa.

Camacho, J.S., Logullo, B.G., Parsekian, G. and Soudias, P.R. (2015). "The Influence of grouting and reinforcement ratio in the concrete block masonry compressive behavior", *Revista IBRACON de Estruturas e Materiais*, 8, 341-364.

Camacho, J.S. and Andolfato, R.P. (2000). "Development of the production techniques of the small scale concrete block", *12th International Brick/Block Masonry Conference*, Madrid-Spain.

CSA Standard A165. (2002). *Concrete materials and methods of concrete construction, methods of test for concrete*, Canadian Standards Association, Toronto.

Drysdale, R.G., Hamid, A.A. and Baker, L.R. (1994). *Masonry structures: Behavior and design*, Prentice-Hall, Englewood Cliffs, N.J.

Eshghi, S. and Pourazin, Kh. (2009). "In-plane behavior of confined masonry walls, with and without opening", *International Journal of Civil*

Engineering, 7(1), 49-60.

Eurocode 6-1996-1-1, 1996-3. (2006). *Design of masonry structures, Part 1-1: Rules for reinforced and unreinforced masonry, Part 3: Simplified calculation methods for unreinforced masonry structures*, European Committee for Standardization, Brussels.

Gustavo, H., Carol. F. and Leonardo, G. (2019). "Strength and failure mechanisms of masonry prisms under compression, flexure and shear: Components' mechanical properties as design constraints", *Journal of Building Engineering*, 28, 101038.

Hamid, A.A., Abboud, B.E. and Harris, H.G. (1985). "Direct modeling of concrete block masonry under axial compression", In *Masonry: Research, Application, and Problems*, ASTM International.

Harris H.G. and Sabnis, G. (1999). *Structural modeling and experimental techniques*, CRC press.

Hassanli, R., ElGawady, M.A. and Mills, J.E. (2015). "Effect of dimensions on the compressive strength of concrete masonry prisms", *Advances in Civil Engineering Materials*, 4(1), 175-201.

Hosseinijou, S.A. and Mansour, S. (2021). "Dynamic material flow analysis of cement in Iran: New insights for sustainability of civil infrastructures", *Civil Engineering Infrastructures Journal*, 54(2), 381-403.

Huang, L., Long, L. and Yan, L. (2014). "Compressive strength of double H concrete block masonry prisms", *Journal of Materials in Civil Engineering*, 26(8), 06014019.

Jablonsky, N. (1996). *Mix design for concrete block, proportioning using the fineness modulus method*, The Aberdeen Group, 1-4.

Long, L., Hamid, A. and Drysdale, R.G. (2005). "Small-scale modeling of concrete masonry using half-scale units: A preliminary study", *10th Canadian Masonry Symposium*, Banff Alberta, June 8-12.

Mohammad, G., Eduardo, R., Almir, B. and Roman, H. (2010). "Influence of vertical joint on the mechanical behavior of concrete block masonry", *Engenharia Estudo*, 10(1), 75-80.

Oliveira, R., Martin, G. and Nalon, G.H. (2018). "Influence of blocks and grout on compressive strength and stiffness of concrete masonry prisims", *Construction and Building Materials*, 182, 233-241.

Rai, D.C. (2002). *Review of design codes for masonry buildings*, Indian Institute of Technology, Kanpur, India.

Sathiparan, N., Anjalee, W.A.V. and Kandage, K.K.S. (2016). "The scale effect on small-scale modelling of cement block masonry", *Materials and Structures*, 49(7), 2935-2946.

Standard No. 2800. (2013). *Iranian code of practice for seismic resistant design of building*, 4th Edition, Ministry of Urban and Road Construction, Tehran.

Zahra, T., Thamboo, J. and Asad, M. (2021). "Compressive strength and deformation characteristics of concrete block masonry made with different mortars, blocks and mortar beddings types", *Journal of Building Engineering*, 38, 102213.